



CEITEC

Central European Institute of Technology  
BRNO | CZECH REPUBLIC

## *Journal club: Ramrath et al, 2013*

*C9940 3-Dimensional Transmission Electron Microscopy*  
*S1007 Doing structural biology with the electron microscope*

**May 11, 2015**



EUROPEAN UNION  
EUROPEAN REGIONAL DEVELOPMENT FUND  
INVESTING IN YOUR FUTURE

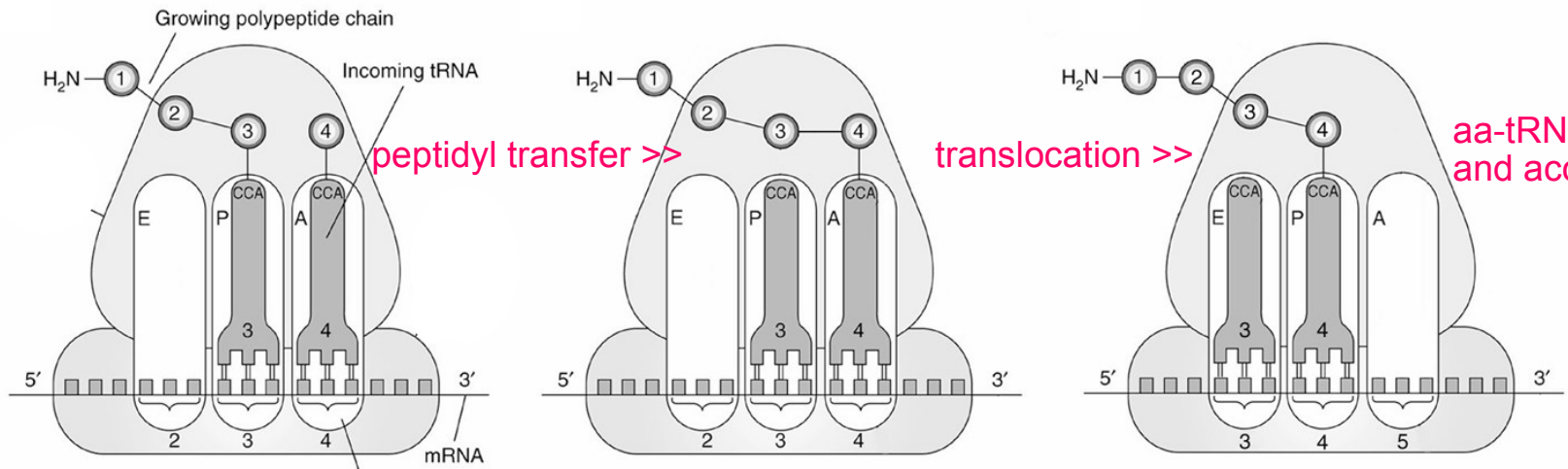


**OP Research and  
Development for Innovation**



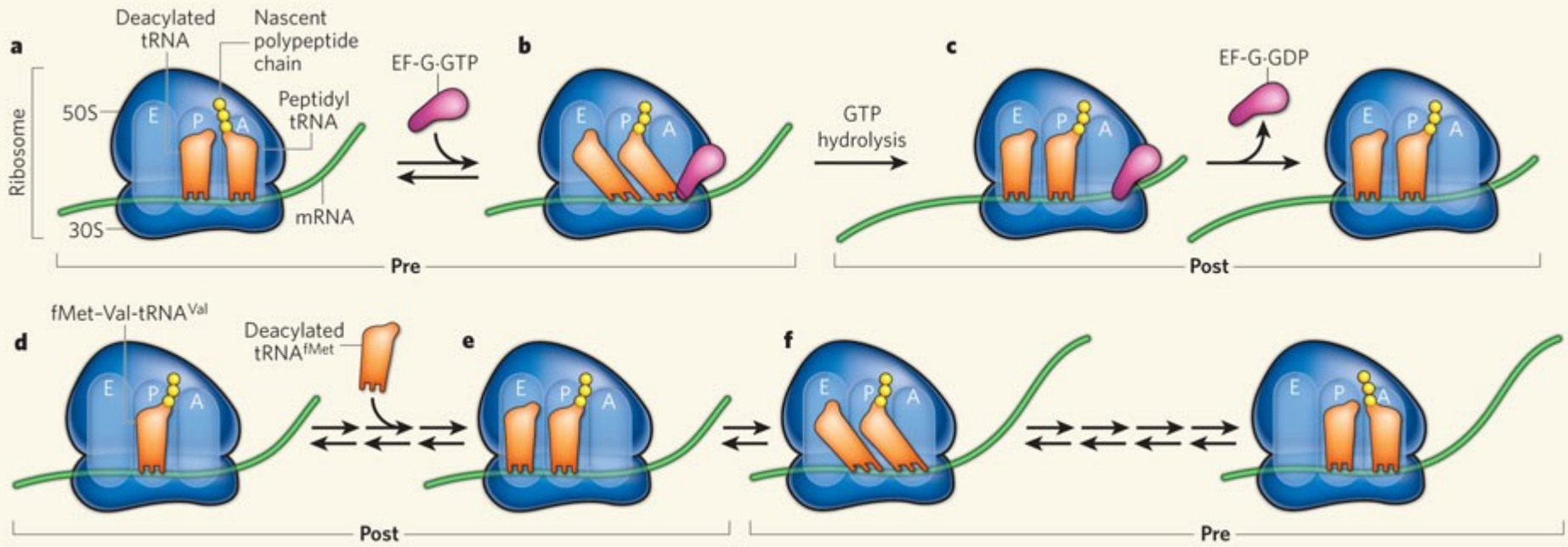
# Elongation of the polypeptide chain by one amino acid

## Large subunit

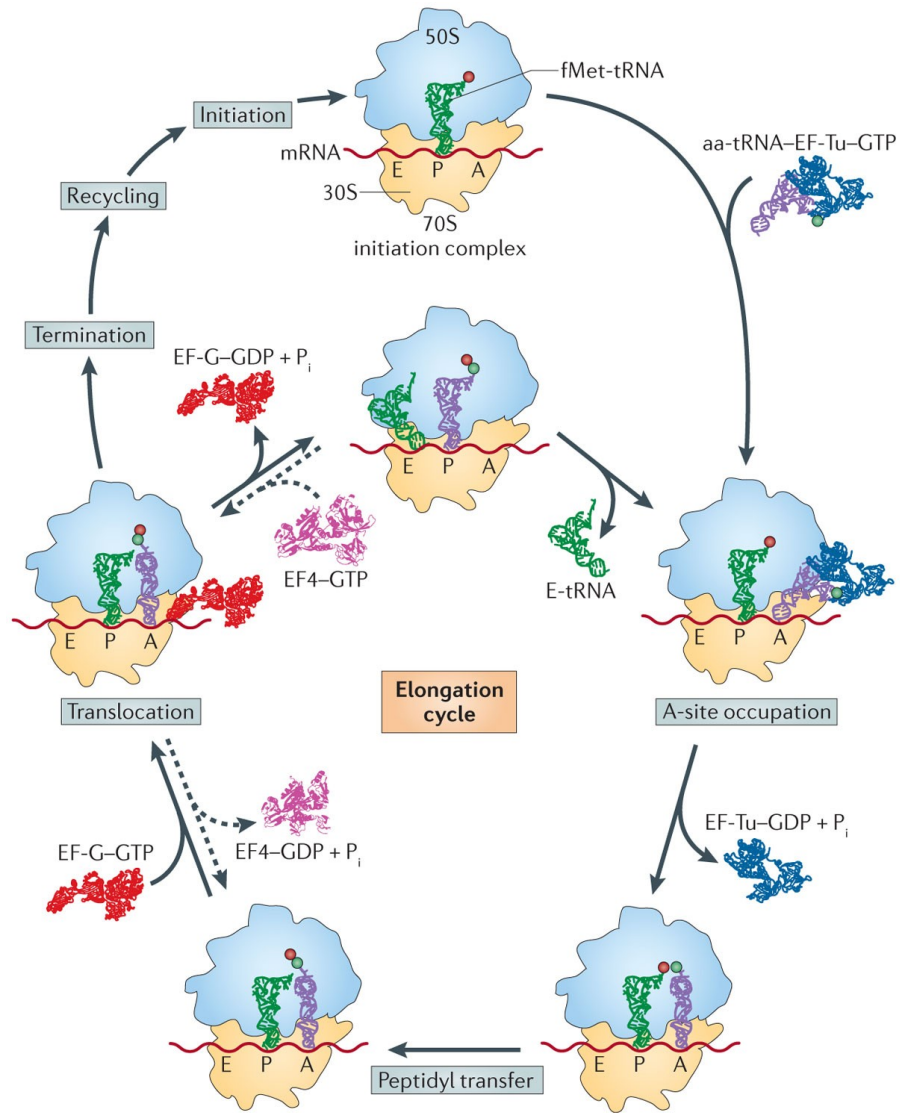


## Small subunit

Adapted from Joachim Frank

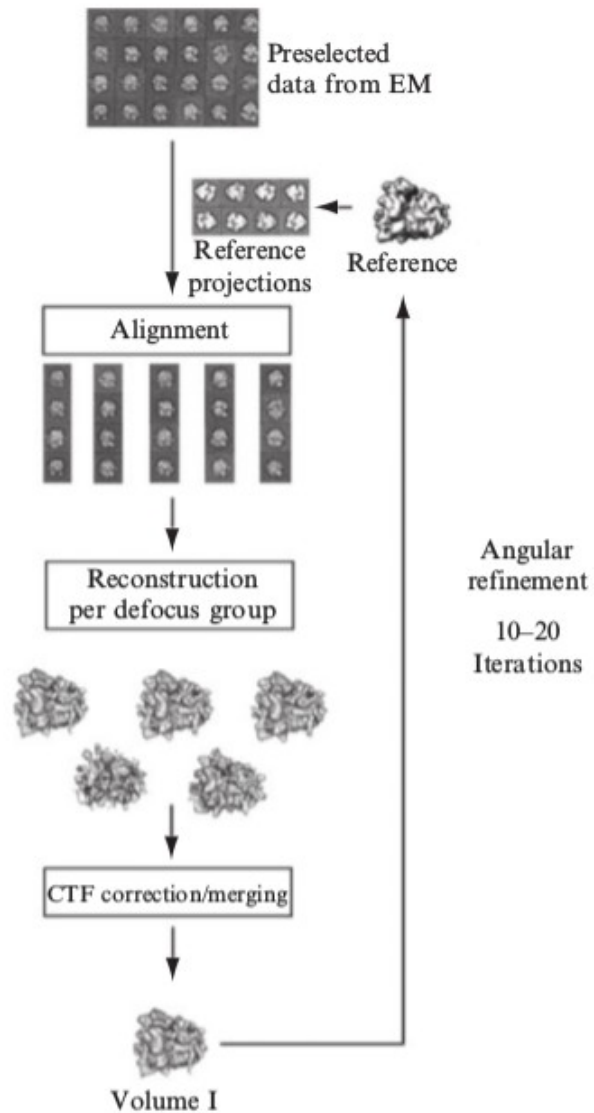


Ehrenberg, Nature, Vol. 466  
Figure 1

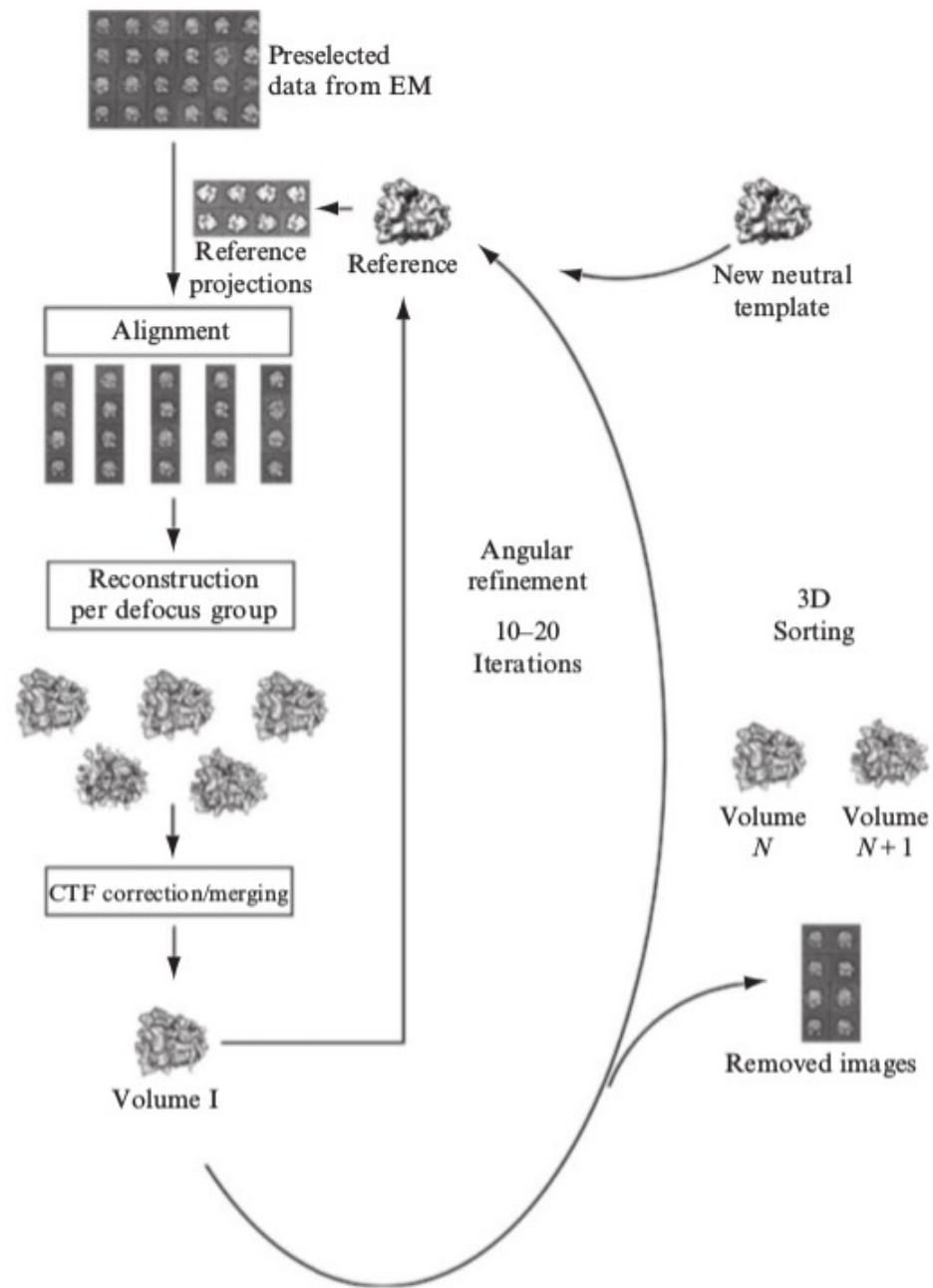


Nature Reviews | Microbiology

Yamamoto et al., (2014) Nature Microbiology, Vol12  
Figure 2



“Normal” reconstruction  
and refinement of orientations



Justus Loerke et al. (2010) *Methods in Enzymology*, Volume 483  
 Figure 2

*Ramrath et al, 2013*

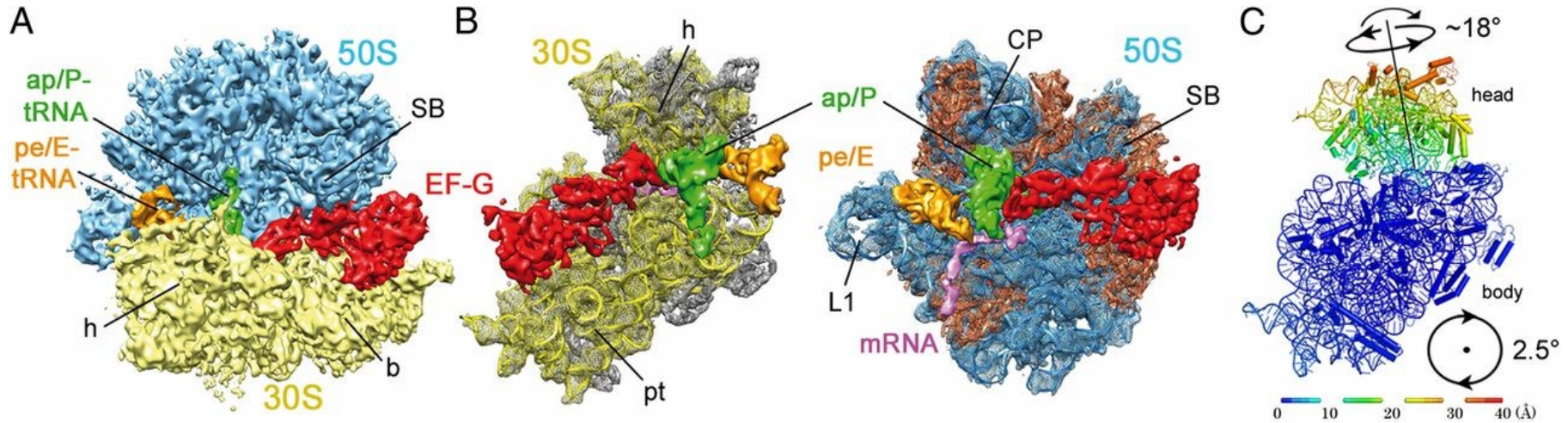
Question:

What's special about this complex?

# Abbreviations used

- ASL: anticodon stem loop
- ASF: A-site finger (Helix H38)

## Overview of the canonical TIPOST complex.



David J. F. Ramrath et al. PNAS 2013;110:20964-20969

Fig. 1. Overview of the canonical TI POST complex. (A and B) Cryo-EM density of the ligands ap/P- and pe/E-tRNAs (green and orange), mRNA (magenta), and EF-G (red) in surface representation within the 70S complex [50S (blue) and 30S (yellow)] (A) or with a mesh representation of both subunits together with docked models of the 30S [16S (yellow) and S-proteins (gray)] and 50S [23S and 5S (blue) and L-proteins (orange)] (B). (C) View from the intersubunit space onto the 30S subunit in the presented authentic TI POST complex. Elements are colored according to their structural displacement compared with the classic conformation (30) upon a common 50S alignment.

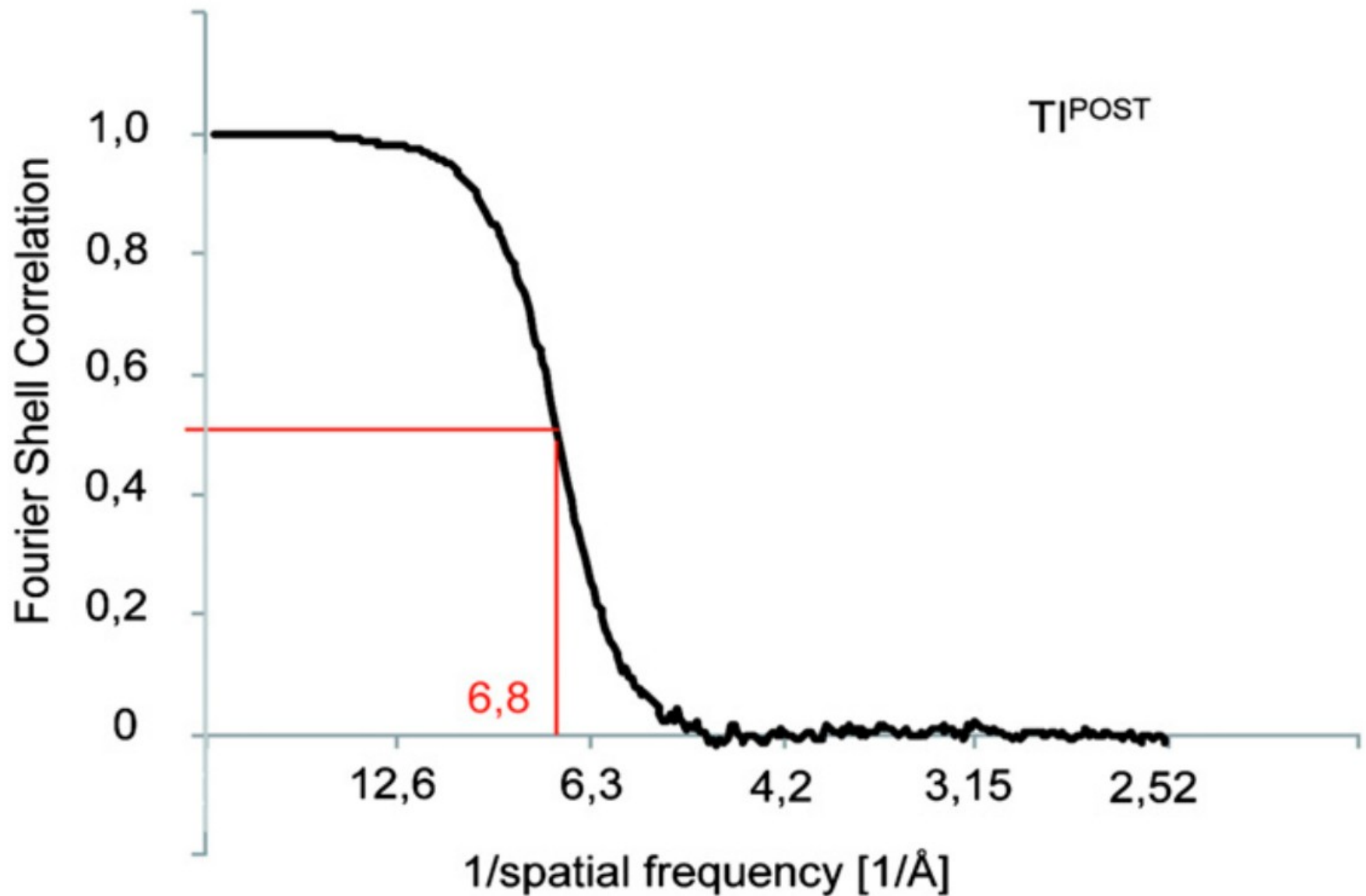
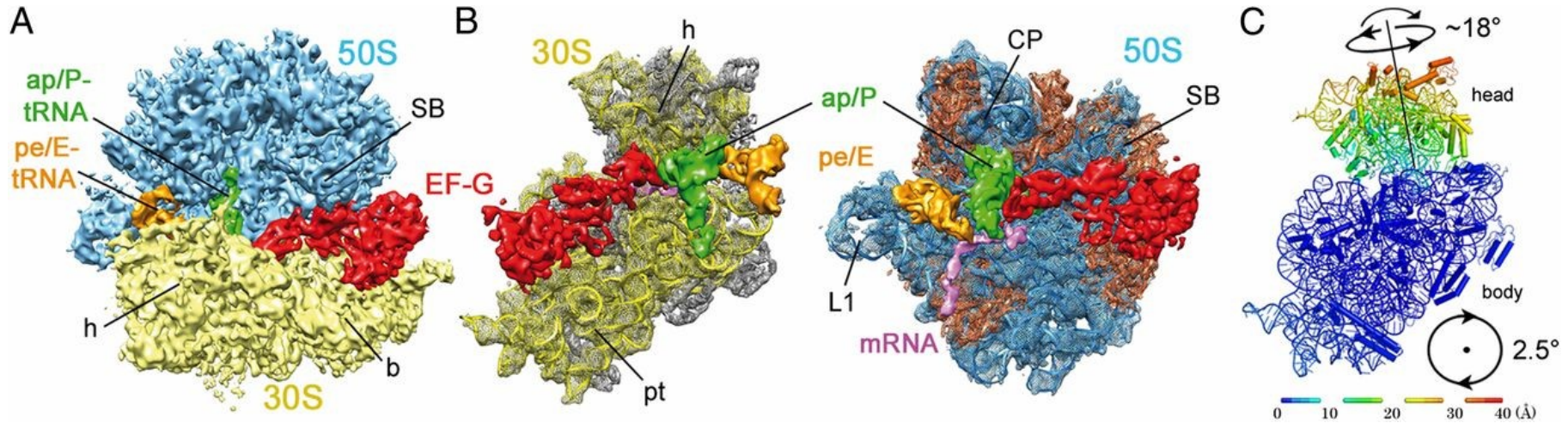


Fig. S1. Resolution curves of the authentic TI POST. According to the 0.5 FSC cut-off, the resolution of the authentic TI POST complex is 6.8 Å.

## Overview of the canonical TIPOST complex.



David J. F. Ramrath et al. PNAS 2013;110:20964-20969

Fig. 1. Overview of the canonical TI POST complex. (A and B) Cryo-EM density of the ligands ap/P- and pe/E-tRNAs (green and orange), mRNA (magenta), and EF-G (red) in surface representation within the 70S complex [50S (blue) and 30S (yellow)] (A) or with a mesh representation of both subunits together with docked models of the 30S [16S (yellow) and S-proteins (gray)] and 50S [23S and 5S (blue) and L-proteins (orange)] (B). (C) View from the intersubunit space onto the 30S subunit in the presented authentic TI POST complex. Elements are colored according to their structural displacement compared with the classic conformation (30) upon a common 50S alignment.

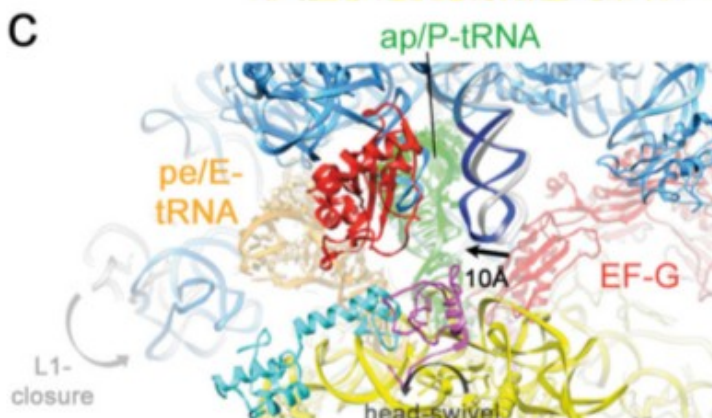
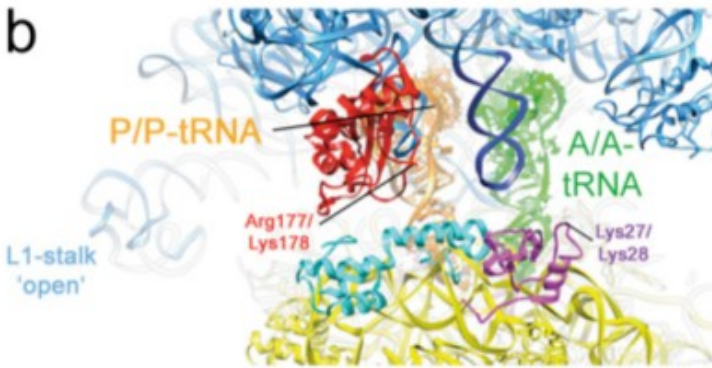
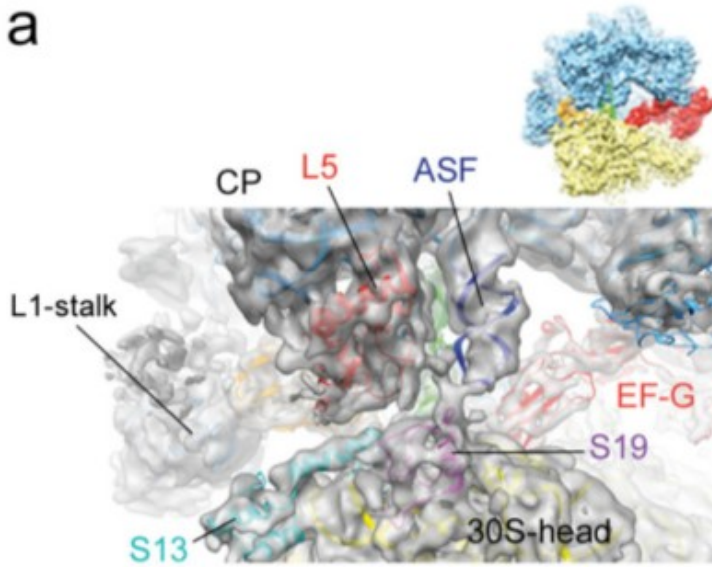


Fig. S2. Formation of a unique intersubunit bridge. (A) Cryo-EM density of the authentic TI POST shown as gray transparent surface with docked models of the ribosome [30S (yellow), 50S (blue), S13 (cyan), S19 (magenta)], EF-G (red), and tRNAs [ap/P-tRNA (green), pe/E-tRNA (orange)]. The map displays a continuous density between L5 (red), the ASF (dark blue), and S19 (magenta). (B) Cartoon representation of the ribosomal conformation in the classic unrotated classic pretranslocational state (15) with an opened L1-stalk indicating the contact between the ASF and S13. (C) Cartoon representation of the authentic TI POST indicating the structural changes of the 30S-head, ASF, and L1-stalk. The positions of L1-stalk and ASF as shown in B are displayed in transparent gray.

David J. F. Ramrath et al. PNAS 2013;110:20964-20969

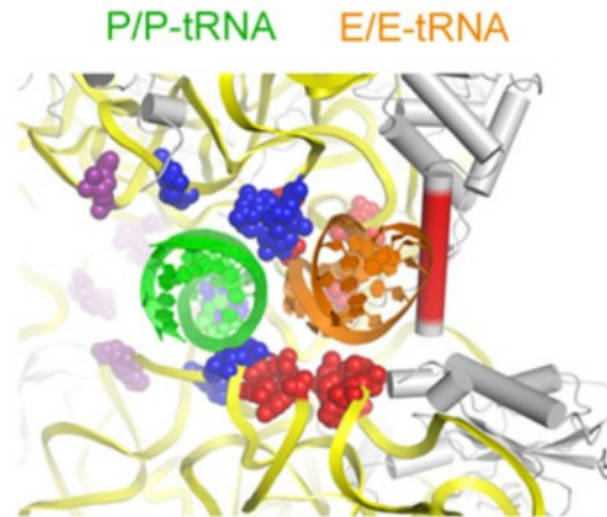
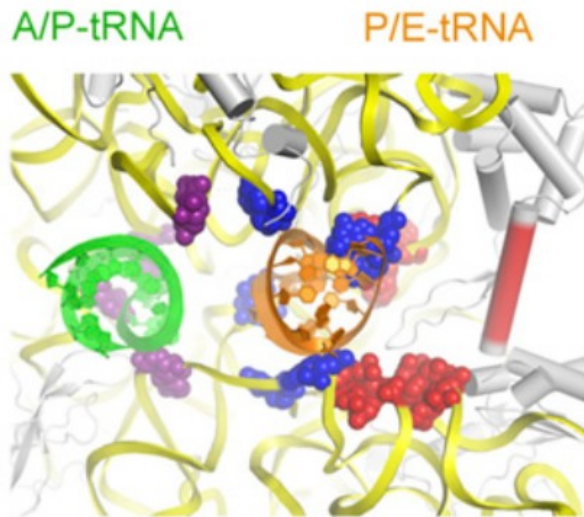
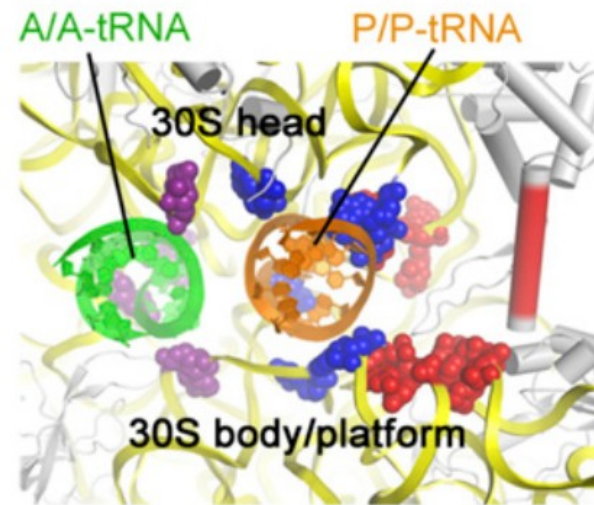
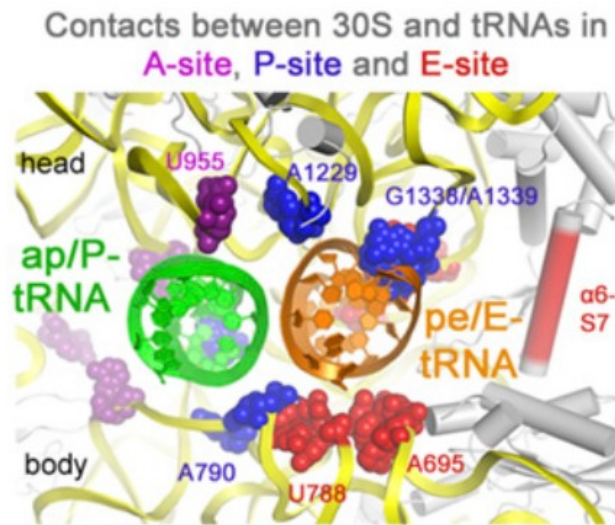
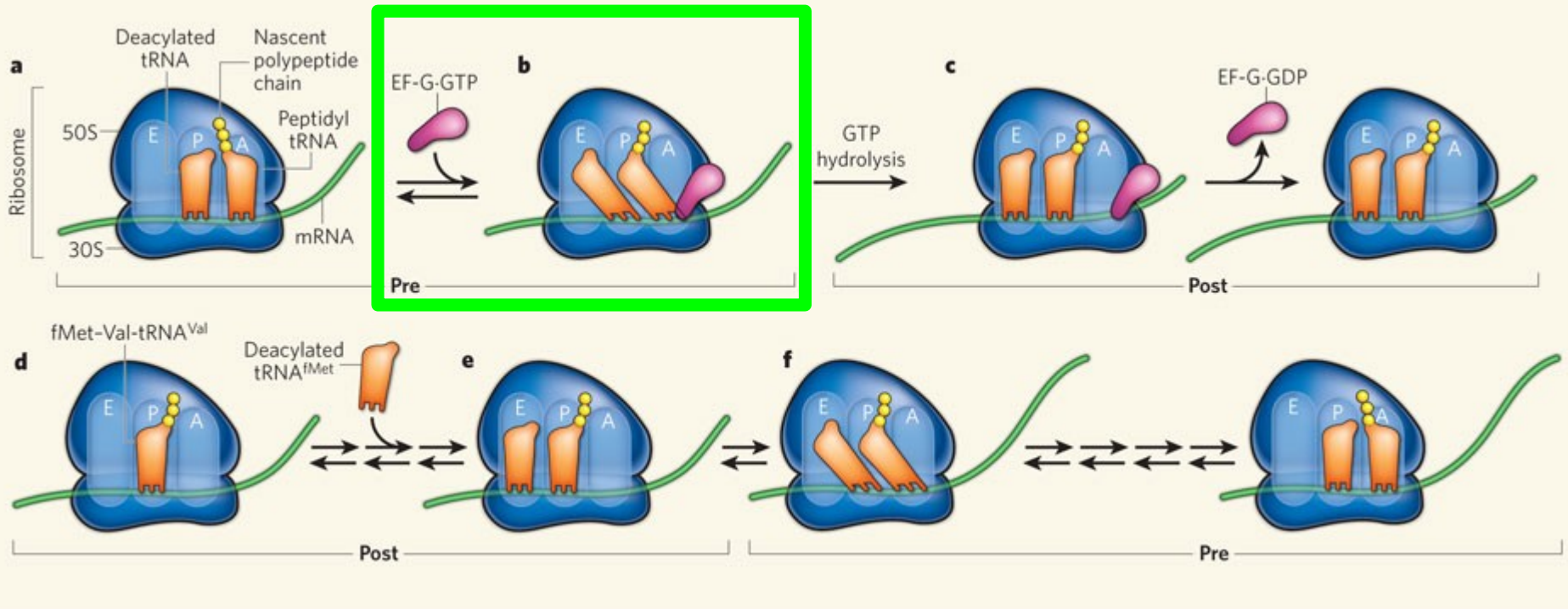


Fig. S3. Interactions of the 30S subunit and different bound tRNAs. Ribbon representation of the tRNA binding region on the 30S subunit. Residues that contact tRNAs in the A (magenta), P (blue), and E site (red) (25) are shown as spheres together with two tRNAs in chimeric intrasubunit (ap/P and pe/E), classic (A/A and P/P), intersubunit hybrid (A/P and P/E), or classic posttranslocated (P/P and E/E) tRNA binding sites (14, 15).



Ehrenberg, Nature, Vol. 466  
Figure 1

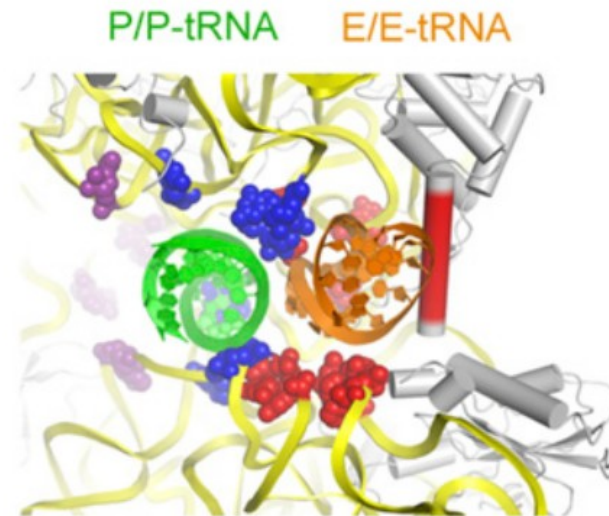
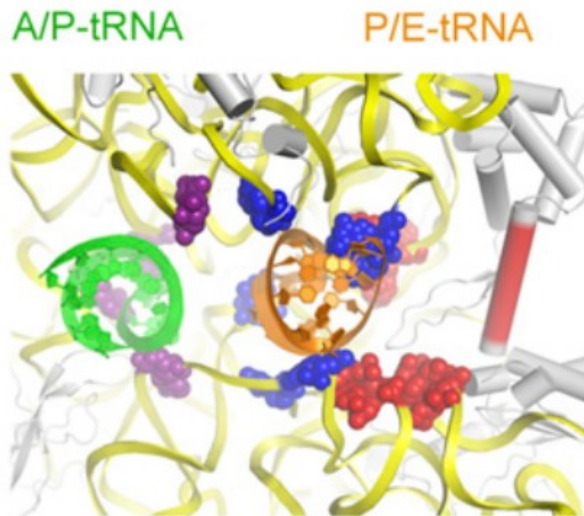
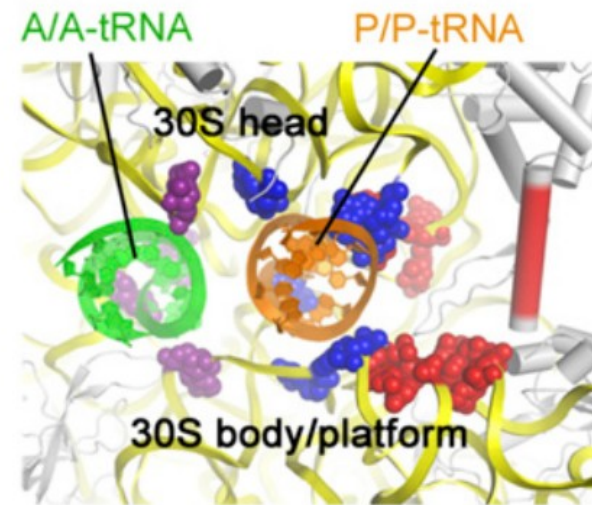
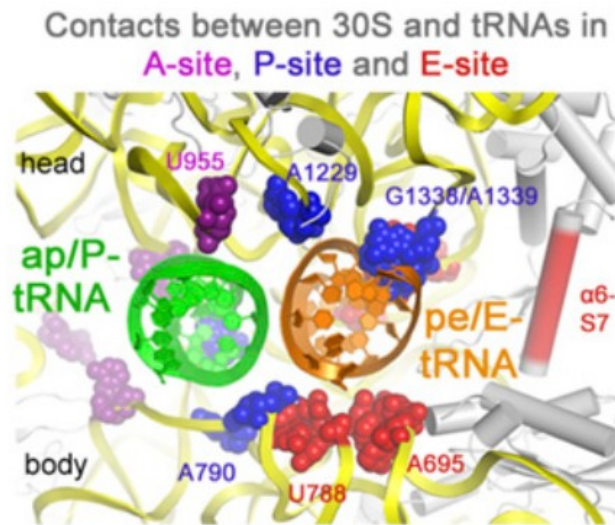
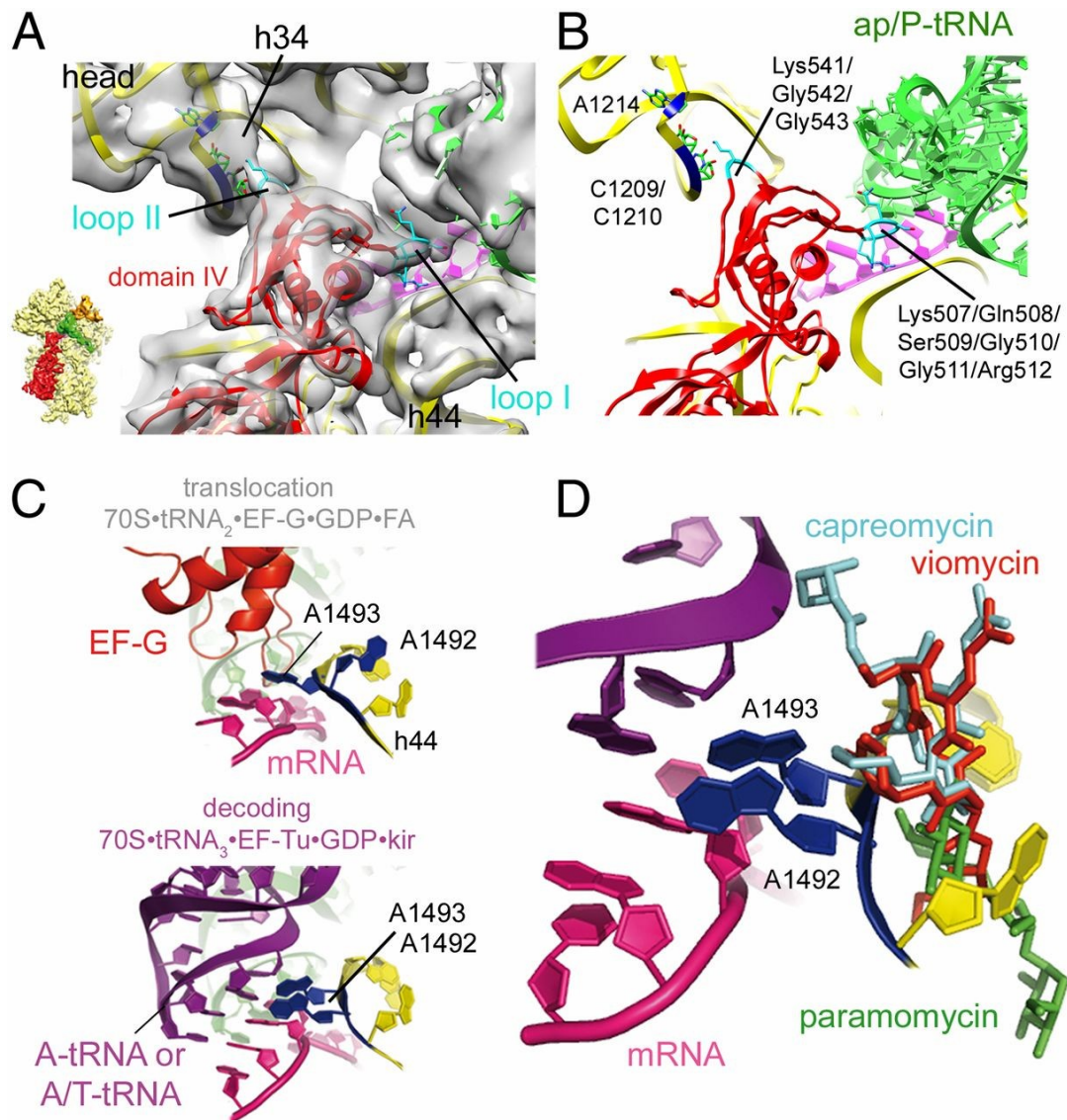


Fig. S3. Interactions of the 30S subunit and different bound tRNAs. Ribbon representation of the tRNA binding region on the 30S subunit. Residues that contact tRNAs in the A (magenta), P (blue), and E site (red) (25) are shown as spheres together with two tRNAs in chimeric intrasubunit (ap/P and pe/E), classic (A/A and P/P), intersubunit hybrid (A/P and P/E), or classic posttranslocated (P/P and E/E) tRNA binding sites (14, 15).

**Contacts of EF-G domain IV. (A) Cryo-EM density of the presented TIPOST complex shown as transparent gray surface together with docked models of the 30S, mRNA, ap/P-tRNA, and EF-G (colored as in Fig. 1) in the indicated view (Left).**



**Ligand positions within the authentic TIPOST complex.**

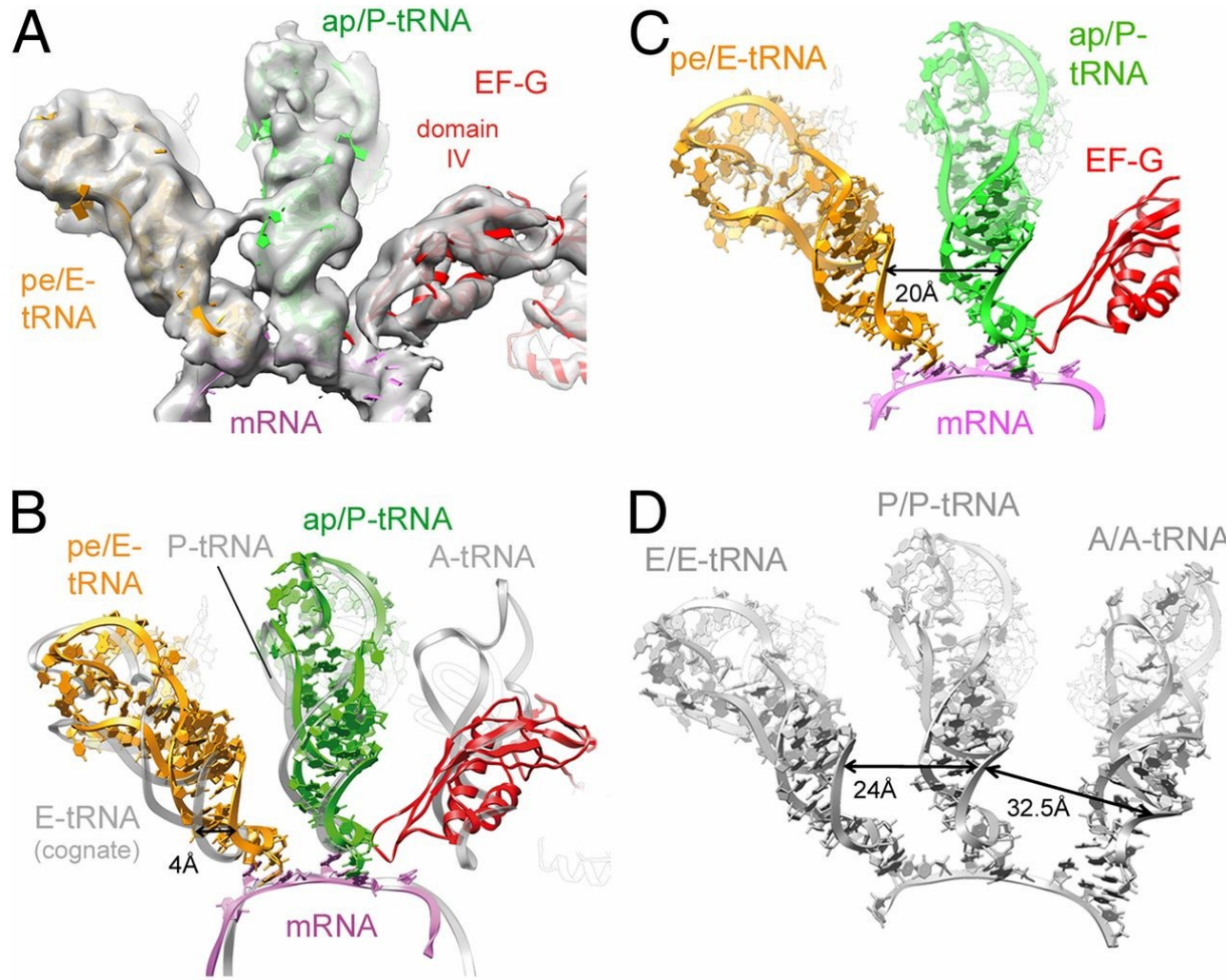


Fig. 3. Ligand positions within the authentic TI POST complex. (A) Cryo-EM density for the ligands within the presented authentic TI POST complex in a transparent surface representation together with docked models of EF-G (red), ap/P-tRNA (green), pe/E-tRNA (orange), and mRNA (magenta). (B) Superimposition of the ligands (as shown in A) together with tRNAs bound to classic A, P, and E sites (transparent gray) (23) upon a 50S alignment. (C and D) Ribbon representation of the ribosomal ligands within the present authentic TI POST complex (C), and an unrotated ribosomal complex with classic A, P, and E-tRNAs (23) (D). Highlighted are the distances between the last base pair within ASL of bound tRNAs.

# Ribosome-tRNA interactions.

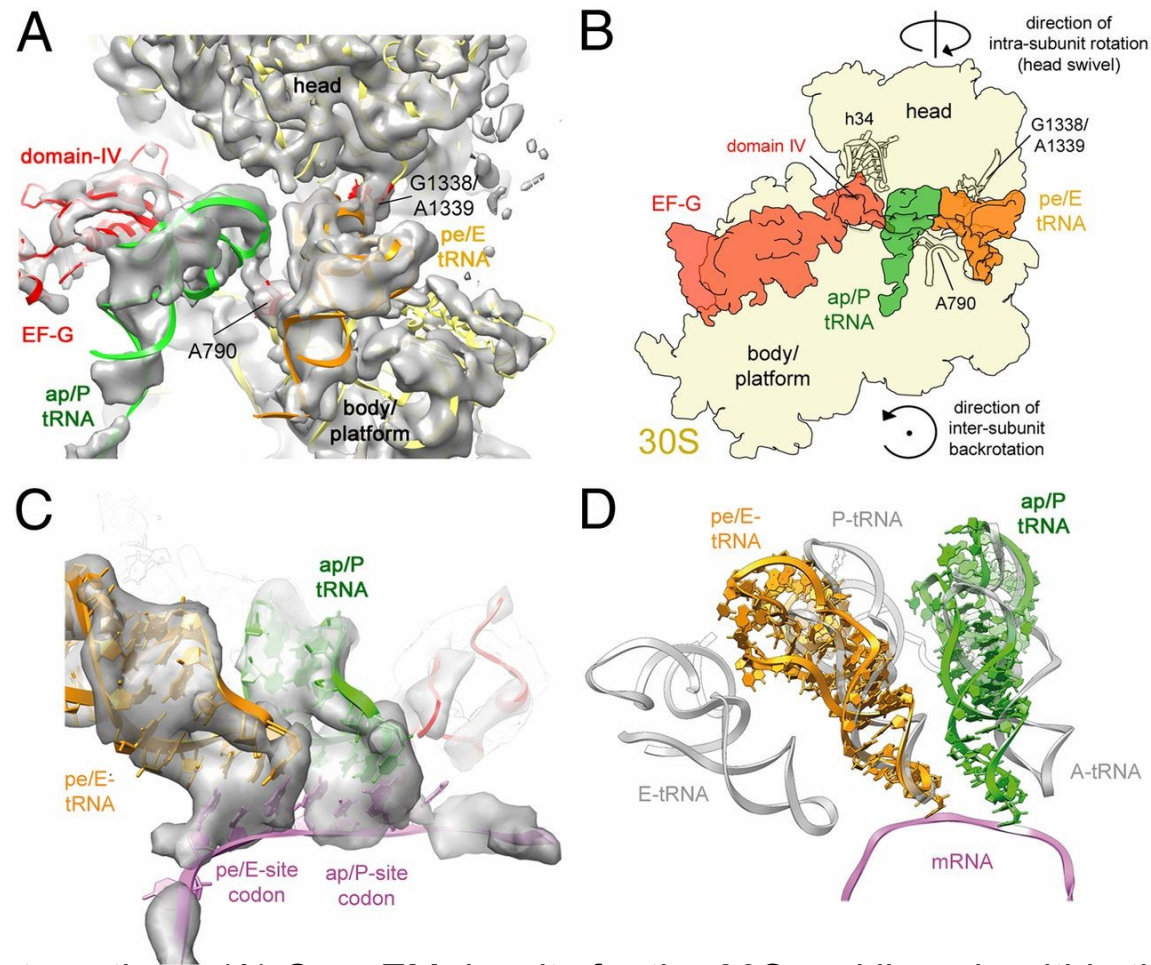
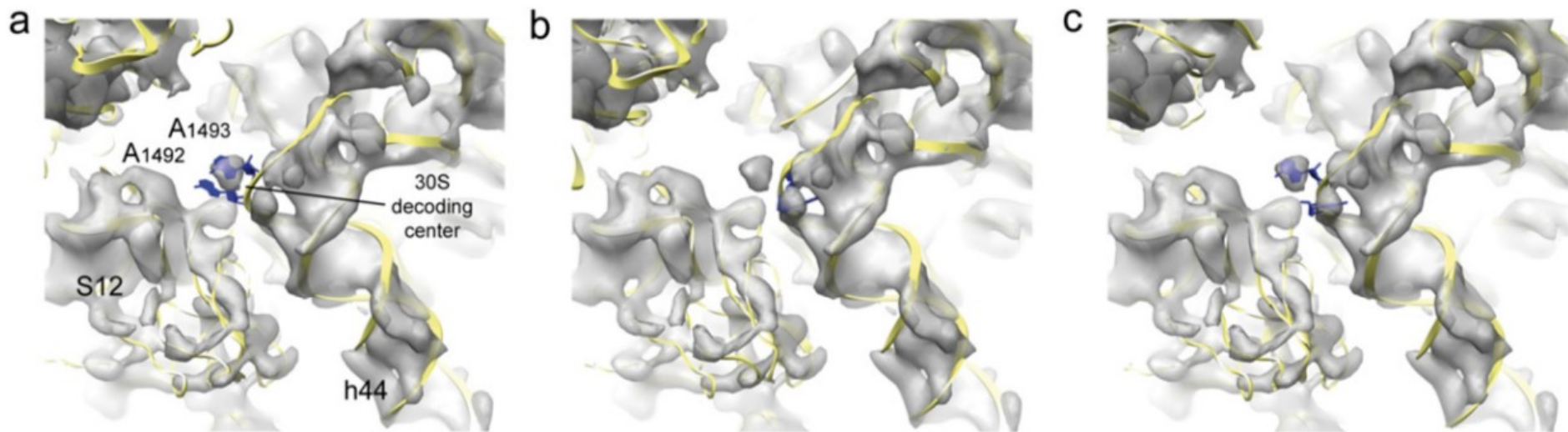


Fig. 4. Ribosome-tRNA interactions. (A) Cryo-EM density for the 30S and ligands within the presented authentic TI POST complex in a transparent gray surface representation together with docked models of the 30S (yellow), ap/P-tRNA (green), pe/E-tRNA (orange), and EF-G (red). (B) Schematic of the 30S subunit and bound ligands [EF-G (red), ap/P-tRNA (green) and pe/E-tRNA (orange)] from the presented authentic TI POST. (C) Cryo-EM density of the ligands within the presented authentic TI POST (transparent gray surface) together with docked models of EF-G, pe/E-tRNA, ap/P-tRNA, and mRNA (colored as in A). (D) Superimposition of the ligands from the present authentic TI POST complex with either tRNAs in classic A, P, and E-site (23) (transparent gray) upon a 30S head alignment.



David J. F. Ramrath et al. PNAS 2013;110:20964-20969  
Supplemental Figure 4

# Thank you for your attention



Central European Institute of Technology  
Masaryk University  
Kamenice 753/5  
625 00 Brno, Czech Republic

[www.ceitec.muni.cz](http://www.ceitec.muni.cz) | [info@ceitec.muni.cz](mailto:info@ceitec.muni.cz)



EUROPEAN UNION  
EUROPEAN REGIONAL DEVELOPMENT FUND  
INVESTING IN YOUR FUTURE



OP Research and  
Development for Innovation

